8. Monteyne R, Comhaire F. The thermographic characteristics of varicocele: an analysis of 65 positive registrations. *Br J Urol* 1978;50:118–120.
9. Dubin L, Amelar RD. Varicocele size and results of varicocelectomy in selected subfertile men with varicocele. *Fertil Steril* 1970;21:606–609.
10. Fariss BL, Fenner DK, Plymate SR, Brannen GE, Jacob WH, Thomason AM. Seminal characteristics in the presence of a varicocele as compared with those of expectant fathers and prevasectomy men. *Fertil Steril* 1981;35:325–327.
11. Bsat FA, Masabni R. Effectiveness of varicocelectomy in varicoceles diagnosed by physical examination versus doppler studies. *Fertil Steril* 1988;50:321–323.
12. Comhaire F, Kunnen M. Selective retrograde venography of the internal spermatic vein: a conclusive approach to the diagnosis of varicocele. *Andrologia* 1976;8:11–24.
13. Ahleberg NE, Bartley O, Chidekel N. Retrograde contrast filling of the left gonadal vein. *Acta Radiol (Diagn)* 1965;3:385–389.
14. Riedel P. Radiological anatomy of the left testicular vein in varicocele and male infertility. In: Jecht EW, Zeitler E, eds. *Recent advances in diagnosis and therapy*. Berlin: Springer-Verlag, 1982:49–52.
15. Freund J, Handelsman DJ, Bautovich GJ, Conway AJ, Morris JG. Detection of varicocele by radionuclide blood-pool scanning. *Radiology* 1980;137:227–230.
16. Harris JD, McConnell BJ, Lipshultz LI, McConnell RW, Conoley PH. Radioisotope angiography in diagnosis of varicocele. *Urology* 1980;16:69–72.
17. Geatti O, Gasparini D, Shapiro B. A comparison of scintigraphy, thermography, ultrasound and phlebography in grading of clinical varicocele. *J Nucl Med* 1991;32: 2092–2097.
18. Ramanna L, Waxman AD, Yoon J, Hyun M. Evaluation of scrotal varicocele with blood-pool scintigraphy, correlation with contrast gonadal venography. *Radiology* 1990;177:143.
19. Lund L, Nielsen AH. Color doppler sonography in the assessment of varicocele testis. *Scand J Urol Nephrol* 1994;28:281–285.
20. Dhabuwala CB, Hamid S, Moghissi KS. Clinical versus subclinical varicocele: improvement in fertility after varicocelectomy. *Fertil Steril* 1992;57:854–857.

Automatic Three-Dimensional Matching of CT-SPECT and CT-CT to Localize Lung Damage After Radiotherapy

Stefan L.S. Kwa, Jacqueline C.M. Theuws, Marcel van Herk, Eugène M.F. Damen, Liesbeth J. Boersma, Paul Baas, Sara H. Muller and Joos V. Lebesque

Departments of Radiotherapy, Nuclear Medicine and Pulmonary Medicine, The Netherlands Cancer Institute, Antoni van Leeuwenhoek Huis, Amsterdam, The Netherlands

The aim of this study was to develop a fast and clinically robust automatic method to register SPECT and CT scans of the lungs. **Methods:** CT and SPECT scans were acquired in the supine position from 20 patients with healthy lungs. After partial irradiation of the lungs by radiotherapy, the scans were repeated. Two matching methods were compared: a conventional method with external skin markers and a new method using chamfer matching of the lung contours. In the latter method, a unique value for the SPECT threshold, needed for segmentation of the SPECT lungs, was determined by iteratively applying the chamfer matching algorithm. **Results:** The new technique for CT-SPECT matching could be implemented in a fully automatic manner and required less than 2 min. No large systematic shifts or rotations were present between the matches obtained with the marker method and the lung contour method for healthy or partially irradiated lungs. For healthy lungs, the number of ventilation SPECT counts outside the CT-defined lung was taken as a measure for a good match. This number of outside counts was slightly lower for the new method than for the conventional method, which indicates that the accuracy of the new method is at least comparable to the conventional method. For ventilation, a systematic difference between the results of the matching methods, a small translation in the anterior → posterior direction, could be attributed to an inconsistency of the marker positions (2 mm). For perfusion, a somewhat larger anterior → posterior shift was found, which was attributed to the gravity force. CT-CT correlation on the lung contours using chamfer matching was tested with the same dataset. For accurate matching, the CT slices encompassing the diaphragm had to be deleted. **Conclusion:** The new method based on lung contour matching is a fast, automatic procedure and allows accurate clinical follow-up.

Key Words: SPECT; CT; lung; image registration; chamfer matching

J Nucl Med 1998; 39:1074–1080

In nuclear medicine, radiotherapy and oncology, there is a growing interest in combining the information of SPECT and CT or magnetic resonance scans. SPECT is used to map organ function and metabolism and has also been established as useful in the evaluation of tumor staging with radiolabeled monoclonal antibodies (*1,2*). One drawback is that SPECT reveals little anatomical information. In contrast, CT gives accurate anatomical detail but does not provide much information about the function of the tissue. The combination of SPECT and CT can, therefore, lead to a more accurate tumor localization or the exact localization of nonfunctioning tissue (*3*). In recent developments in radiotherapy, lung SPECT is combined with CT. Here, regions of nonfunctional lung tissue are identified with perfusion and ventilation SPECT scans, which gives additional information for the design of a radiation treatment plan based on the CT scan (*4*). Furthermore, it has been shown that lung SPECT is a very sensitive method for monitoring radiation damage after radiotherapy, if it is combined with CT (*5,6*). Of course, the prerequisite for an optimal combination of the information of the different modalities is that the SPECT and CT scans need to be matched spatially (i.e., registered). For clinical application, the matching method should be fast and robust.

In a research project to establish the dose–effect relationship for lung tissue after radiotherapy, several hundred CT-SPECT registrations have to be performed. Previously, the CT-SPECT matching was performed using external markers placed on the skin (*5*). The registration of the scans was performed by minimizing the root mean-square (RMS) distance between the markers. This method has several disadvantages. For the different modalities (CT or SPECT), different markers have to be used. This procedure is inaccurate due to the variation in the positioning of the markers. The markers have to be identified in both scans, which is done manually and is time-consuming. The skin (and markers) can also move with respect to the organ of

Received May 13, 1997; accepted Sep. 3, 1997.
For correspondence or reprints contact: Stefan L.S. Kwa, PhD, Department of Radiotherapy, The Netherlands Cancer Institute, Antoni van Leeuwenhoek Huis, Plesmanlaan 121, 1066 CX Amsterdam, The Netherlands.

interest (lungs), depending of the exact position of the patient. Especially in follow-up studies taking place on a time scale of months or years, the weight loss or gain will have a large influence on the skin position with respect to the organ of interest. It has been reported that, recognizing these limitations, it is necessary to improve the image match manually by visually superimposing the CT lung contours on the SPECT dataset (*6*). Instead of matching the lung contours manually, it would be more convenient and faster to perform this operation automatically. An additional advantage is that, because no markers are needed, CT and SPECT scans can be matched retrospectively.

Several optimization algorithms have been reported to match three-dimensional surfaces of different modalities (*7–11*). The surface-fitting algorithm developed by Pelizzari and Chen (*7*) and Kessler et al. (*8*) has been applied for the matching of CT and PET thorax scans by Yu et al. (*12*). They found that the pleural surfaces of the lungs obtained from the CT scan and the transmission image set of the PET scan are suitable to perform the registration. Another algorithm is chamfer matching, which has been applied successfully for the brain in CT-CT, CT-SPECT, CT-MRI and MRI-PET (*9–11*). This algorithm is faster and imposes less strict demands on the complexity and quality of the organ contours. Because of the latter property, lung contour extraction can be kept very simple and can, therefore, be expected to be performed without user interaction.

Because the chamfer matching algorithm has been shown to be very accurate for CT-SPECT matching of the brain, as mentioned above (*11*), it can be expected to be also the case for other, nonmoving organs. However, for the validation of this technique for the lungs, several aspects have to be verified. The breathing motion during scans and differences in breathing level between the two scans could induce errors in the match. Second, it has been reported that the lung apices show fewer SPECT signals than do the other lung regions (*13*), which could cause a systematic shift when lung contours are matched. Also, reduced function after radiotherapy, particularly, lung regions (*5*), could induce this problem. Third, lung SPECT exhibits a lower spatial resolution than brain SPECT, mainly due to differences in collimator type and geometry, which could influence the accuracy of the registration.

We aim to customize the chamfer matching technique for the registration of lung contours, such that the whole process is fully automatic, including threshold determination and extraction of the lung contours. We evaluated the robustness of chamfer matching in the clinic. Due to the physiological nature of the possible pitfalls under investigation, our study was performed with human subjects rather than with a phantom. This work is based on the scans of 20 patients, before and after radiotherapy, for which the new method was compared with the conventional method using external skin markers. Using the same data, CT-CT lung contour matching was also tested. The latter test will become relevant for the registration of CT and transmission scans, recorded on the gamma camera during SPECT or PET acquisition.

MATERIALS AND METHODS

Patients

In this study, the images of 20 patients with healthy lungs, who underwent radiotherapy for malignant lymphoma, were used (*5*). The patients were irradiated with a mantle field, i.e., 30%–50% of the lung volume was irradiated. The maximum total dose in the lung was 35–45 Gy.

Data Acquisition

Before radiotherapy and 3–4 mo after radiotherapy, a CT thorax and a lung SPECT scan were obtained (*13*). For SPECT, a dual-head gamma camera (ADAC Genesis or ADAC Vertex), equipped with medium-energy, general-purpose collimators, was used. The scans were recorded in the dual-isotope acquisition mode with ^{81m}Kr and ^{99m}Tc, and the ventilation and perfusion were measured simultaneously (scan time ≅15 min). The patient was lying supine with the arms raised above the head. The CT scan was made within 1 wk of the accompanying SPECT scans, with the patient in the same position (Somatom Plus scanner; Siemens). Both CT and SPECT acquisition were performed under normal breathing conditions (no "breath-and-hold" procedure). The CT scan time was typically 10 min, depending on the number of slices, and the exposure time per slice was 1.0 sec. Both the SPECT and the CT scan included the entire lung volume. CT slices were recorded every 10 mm (8-mm slice thickness), yielding 20–30 slices, and the number of pixels per slice was 512 × 512 (pixel size, typically 1 mm). SPECT scans were reconstructed using filtered backprojection, without attenuation correction, with software provided by the manufacturer (ADAC). The number of voxels was 64 × 64 × 64, and the voxel size was approximately 6 mm. The resolution of the reconstructed SPECT images was 20–25 mm FWHM, as measured with a line source filled with ^{99m}Tc.

CT-SPECT Matching Using Markers

Five external skin markers were used to align the SPECT scans with the accompanying CT scan. The exact points were indicated with ink on the chest, abdomen, left and right lateral sides and back. These skin positions were subsequently marked with ^{57}Co point sources during SPECT scanning and with crossed radio-opaque catheters during CT scanning. Each ^{57}Co point source (diameter = 2 mm) was encapsulated in the center of a perspex disk (i.e., cylinder height = 6.0 mm, diameter = 25.4 mm). The five skin positions were identified visually in the SPECT and CT scans, and the RMS distance between the corresponding markers was minimized by allowing translations and rotations.

CT-SPECT: Lung Contour Matching

Contour Extraction. The 512 × 512 CT images were converted to a 256 × 256 format by omitting three-quarters of the pixels (no averaging), thereby leaving the gray value histogram intact. The CT images were segmented by binary thresholding. The threshold value was chosen at a density of 0.7 g/ml, which is approximately in the middle of the transition from lung tissue (~0.3 g/ml) to water (1.0 g/ml). For each slice, all contours were traced, and the contour enclosing the largest area (body contour) was deleted. The result was a list of contour points. In the matching procedure, the number of points was limited to 5000 by resampling for efficiency purposes.

The ventilation and perfusion SPECT scans were also segmented by binary thresholding. Contour tracing was also done slice by slice, again with a maximum of 5000 contour points.

Chamfer Matching. The method of chamfer matching was applied using the software modules as described elsewhere (*11*). The method uses the lists of contour points of a structure/organ, extracted from each scan. One of the scans, in our case, the CT scan, is chosen to be the template. For this scan, a distance transform is calculated from the extracted contour points. A generalized city-block distance for nonequidistant slices was used (*11*), and the CT grid was taken as the calculation grid. Optimization of the match was done by minimizing a cost function, calculated from the distance transform and the SPECT contour points, and allowing translations and rotations of the SPECT scan. The RMS cost function was applied, which is the most commonly applied measure for the goodness of fit between two geometrical shapes (*11*). It is a measure for the RMS distance between the contour points of the SPECT and CT scan (*11*). The RMS cost

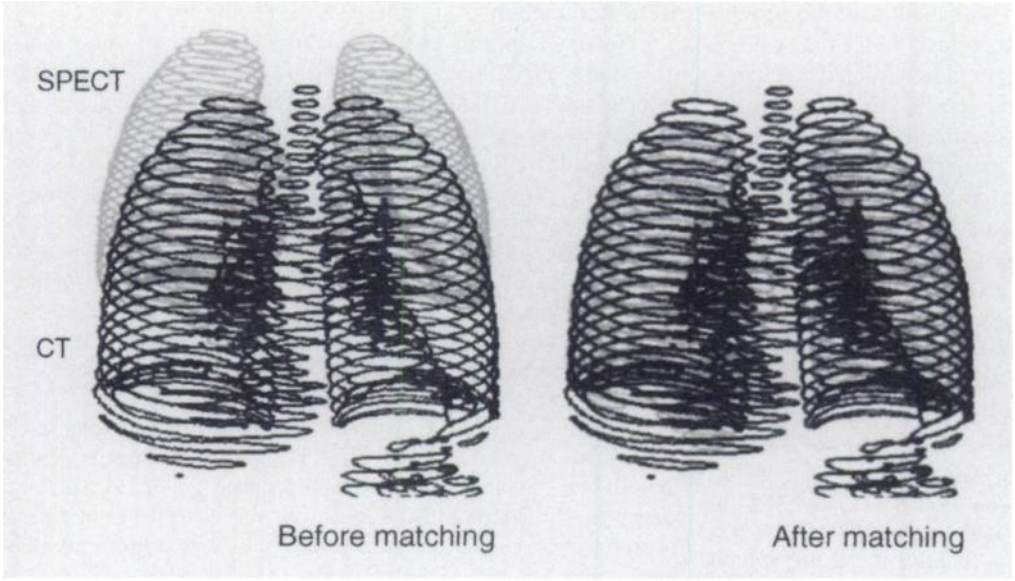

FIGURE 1. Three-dimensional view of the lung contours extracted from CT (black) and ventilation SPECT (gray) scans. (Left) Before lung contour matching. (Right) After lung contour matching. Note that it was not necessary to remove the contoured features present in the CT and absent in the SPECT scan, such as the trachea and air in the stomach/bowel.

function was preferred over the mean cost function (*11,14*) because the SPECT threshold and, thus, the size of the SPECT lung surface were not known a priori. For the matching of two objects with incompatible magnification factors, the mean cost function is expected to give solutions that are not unique. Additionally, RMS performs better in the presence of global shape differences, when no outliers are present (*14*).

Iterative SPECT Threshold Determination. The threshold used for the segmentation of the SPECT scan was difficult to assess beforehand. As a starting value, an arbitrary value of 200 counts was chosen (the maximum count value in the scans was 300–800 counts). Subsequently, the process of chamfer matching was performed, resulting in an initial match. Next, the chamfer matching procedure was repeated for another SPECT threshold until the cost function was minimal. Here, a simple, bisection searching method was used. The stop criterion for iteration was that the step size in the SPECT threshold value was <7 counts. The iteration process could be done within a reasonable amount of time because the distance transform had to be calculated only once from the CT and the number of voxels in the SPECT scan was relatively small (allowing repeated segmentation and contour extraction). No user interaction was required.

CT-CT: Marker/Manual Matching

For the matching of the CT scans before radiotherapy and after radiotherapy, anatomical landmarks, such as the center of a thoracic vertebra, bifurcation of the trachea and the sterno-clavicular joints, were used (*5*). The resulting match was visually checked after superposition of the posttreatment CT lung contours on the pretreatment CT scan. Manual shifting of the scans was applied if necessary.

CT-CT: Lung Contour Matching

The lung contours were extracted from the pre- and post-treatment CT scans as described above. For matching, the pretreatment CT scan was used as the template. When chamfer matching was applied using these lung contours, sometimes mismatches were observed, for example, totally nonoverlapping contours of the tracheas. Because the patient was scanned while continuously breathing, the contours in the slices of the diaphragm were extremely different from scan to scan. By omitting these contours from the post-treatment scan, the mismatches could be avoided.

This extra step was added in the matching procedure by manually deleting all CT slices that contained or were suspected to contain parts of the diaphragm. The lung contours/slices of the pretreatment scan were always left intact. Removing the diaphragm region in the template scan would have had no effect because, in principle, the cost function is not evaluated here, once the match has converged.

RESULTS

CT-SPECT

Performance of the New Method. The method for matching CT and SPECT scans works in a fully automatic manner. Typically, fewer than 10 iterations were necessary to find the optimal SPECT threshold value. A match was performed using the ventilation SPECT and using the perfusion SPECT scan, for each of the 20 CT-SPECT scan pairs recorded before radiotherapy and for the 20 CT-SPECT pairs after radiotherapy. However, for one patient, the ventilation was not measured after irradiation, thus leaving a total of 79 match operations. All registrations were inspected roughly by superimposing the CT lung contours on the SPECT lung contours after the matching process (Fig. 1). No obvious mismatches (e.g., left CT lung matched to the right SPECT lung) were detected.

The calculation times ranged from 45 to 100 sec on a PC (90-MHz Pentium processor, 32 MB memory), i.e., the whole matching procedure requires less than 2 min of computation time, which includes the data access of the scans.

Comparison of the Two Methods. For each CT-SPECT pair, the marker match method (conventional method) and the lung contour method (new method) were applied. The two matches were compared by superimposing the lung contours of the CT and the SPECT scans in three dimensions (Fig. 1) and in two dimensions or by superimposing the segmented CT lungs on the SPECT scan in two dimensions (Fig. 2). In all cases, the new method seemed to result in equal or better match accuracy, as judged visually (subjectively).

For each patient, the transformation matrix obtained with the lung contour method was compared to that obtained with the marker method. The comparison between the two different transformation matrices was made by calculating the difference in translation (ΔT) and the difference in rotation (ΔR) of the lungs. The center of rotation was chosen in the center of the lungs, defined as the center of the smallest box around the lungs. Thus, for each patient i, six numbers were determined: $\Delta T_{AP,i}$, $\Delta T_{CC,i}$, $\Delta T_{RL,i}$, $\Delta R_{AP,i}$, $\Delta R_{CC,i}$ and $\Delta R_{RL,i}$. The indices denote the directions anterior $\rightarrow$ posterior (AP), caudal $\rightarrow$

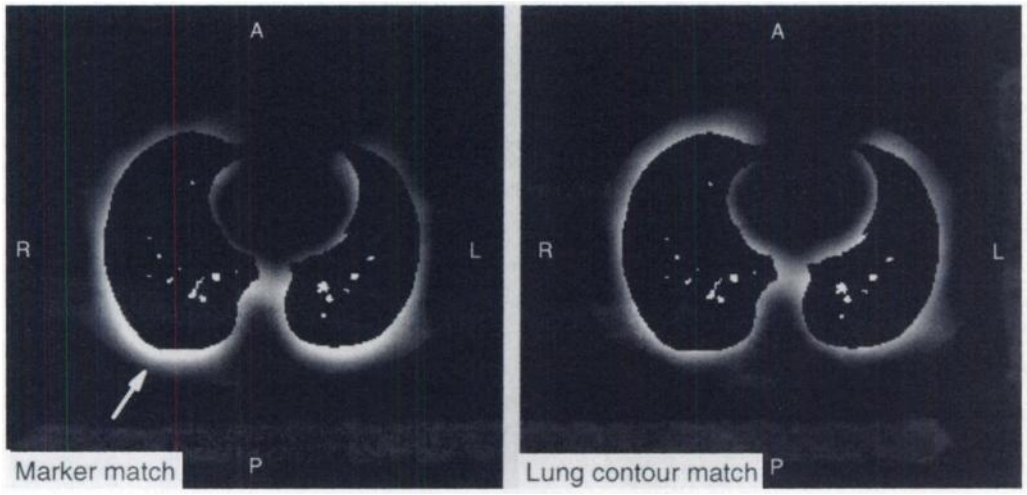

FIGURE 2. Transversal image of SPECT ventilation counts outside the CT-defined lung after CT-SPECT matching. (Left) Marker match. (Right) Lung contour match. Note the increased activity on the posterior side of the lungs (Left, white arrow).

cranial (CC) and right → left (RL). For two identical transformation matrices, these numbers are zero.

Shown in Table 1 are the values we observed (averaged for the 20 patients) for ΔT_{AP}, ΔT_{CC}, ΔT_{RL}, ΔR_{AP}, ΔR_{CC} and ΔR_{RL}, where $\Delta T_{AP} = (\Sigma_i \Delta T_{AP,i})/N$ and so on (N is the number of patients). Also are indicated the s.e.m. values. It can be seen that most values in the table are close to zero, meaning that there are no large systematic differences between the old and the new matching methods.

When looking in more detail, we see that, for CT-SPECT ventilation matching of healthy lungs (i.e., before irradiation, Table 1, first column), only one value is different from zero in a statistically significant manner (>2 s.e.m.; $p < 0.05$), $\Delta R_{AP} = 0.9°$, but the difference is small. For CT-SPECT ventilation matching of irradiated lungs, the results are very similar to those for healthy lungs (compare the first and second columns), except that now only ΔT_{AP} is different from zero in a statistically significant manner. A similar shift is present before irradiation but is not significant. Also for CT-SPECT perfusion matching of healthy lungs (third column) and of irradiated lung (last column) ΔT_{AP} is statistically different from zero. Here, the difference is about −6 mm and comparable to the voxel size of the SPECT scan (6 mm). The negative sign means that the SPECT scan is positioned more anterior when the lung contour method is used than when the marker match method is used.

In summary, before and after irradiation of the lungs, very similar results are obtained. That is, when the ventilation SPECT lung contours are used, no large systematic shifts or rotations are detected between the lung contour method and the marker match method. When the perfusion SPECT lung contours are used, the lung contour method clearly shifts the SPECT scan in the posterior → anterior direction, with respect to the marker match method.

A visual comparison was made between the marker match (Fig. 2, Left) and the lung contour match (Fig. 2, Right) for a particular patient. Shown are the ventilation SPECT counts that are outside the CT-defined lung, after matching (with either method). In the ideal case, there is no SPECT activity in the soft tissue surrounding the lungs. In practice, however, activity is observed in this region due to the relatively low resolution of the SPECT scan due to camera/collimator blurring and photon scatter in the patient. When judging both images by eye, the lung contour match (Fig. 2, Right) seems to be better than the marker match (Fig. 2, Left) because the SPECT counts surrounding the CT-defined lung are more symmetrically distributed (e.g., note the hot regions, indicated by the white arrow, at the posterior side in the marker match image).

The number of SPECT ventilation counts outside the CT-defined lung ($N_{outside}$) and the total number of ventilation counts in the three-dimensional SPECT scan (N_{total}) were quantified for the patients with healthy lungs (i.e., before radiotherapy). For the patient in Figure 2, $N_{outside}$ was smaller for the lung contour match than for the marker match. This property was observed for almost all other patients (except for

TABLE 1
Average Transformation Between Marker Match and Lung Contour Match*

Parameter	Ventilation		Perfusion	
	Before irradiation	After irradiation	Before irradiation	After irradiation
Translation, mean ± s.e.m. (mm)				
ΔT_{AP}	−1.6 ± 0.9	−2.6 ± 0.8	−5.5 ± 0.9	−7.0 ± 1.0
ΔT_{CC}	0.0 ± 1.6	−2.1 ± 2.2	1.4 ± 1.8	0.7 ± 2.9
ΔT_{RL}	0.5 ± 0.5	0.7 ± 0.9	0.6 ± 0.6	1.3 ± 1.0
Rotation, mean ± s.e.m.				
ΔR_{AP}	0.9 ± 0.2	−0.5 ± 0.4	0.2 ± 0.6	0.4 ± 0.9
ΔR_{CC}	−0.1 ± 0.3	−0.1 ± 0.4	0.7 ± 0.7	0.4 ± 0.5
ΔR_{RL}	−1.2 ± 0.8	1.0 ± 1.1	−1.3 ± 0.9	1.5 ± 0.8
No. of patients	20	19	20	20

*For each patient, the CT and SPECT scans were matched with the two methods, yielding two transformations for the SPECT scan (the CT was the template). Presented are the differences between these transformations (three translations and three rotations, ΔT and ΔR, respectively), averaged for 19 or 20 patients. The indices denote the axis directions anterior → posterior (AP), caudal → cranial (CC) and right → left (RL). Also indicated are the s.e.m. values. The signs are defined such that the numbers represent the transformation (of the SPECT scan) from the marker match situation to the lung contour match situation. If the marker match had been identical to the lung contour method, all values would be zero.

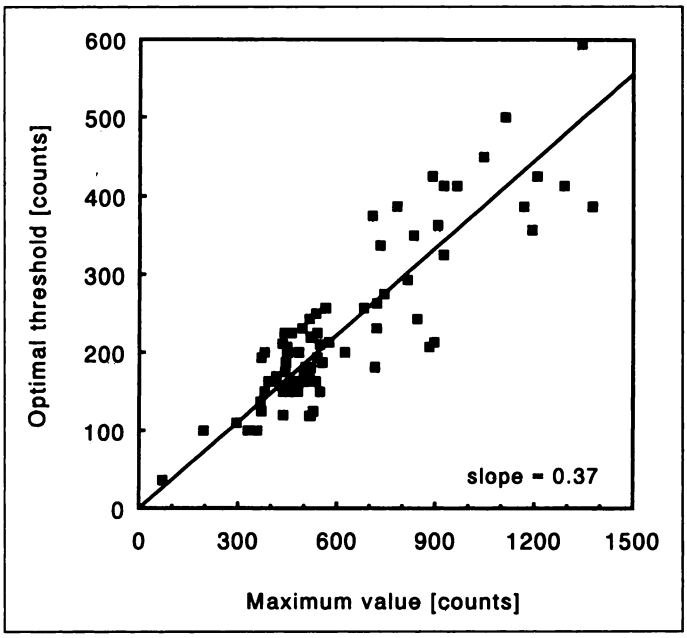

FIGURE 3. Optimal SPECT threshold as a function of the scan maximum (ventilation), determined for 81 patients with healthy lungs. The optimal SPECT threshold was found with CT-SPECT matching by iteratively applying the lung contour match (automated, new method). The data could be fitted with a straight line through the origin (slope = 0.37 ± 0.01, ± s.e.m.).

one patient, for whom the counts were almost the same). On average, $N_{outside}/N_{total}$ was 1.1% ± 0.2% (mean ± s.e.m.) smaller for the lung contour match than for the marker match. Although the difference is small, it is statistically significant.

Optimal SPECT Threshold. Our database contained the CT and ventilation SPECT scans of 81 patients (42 lymphoma patients and 39 breast cancer patients), which were measured before radiotherapy. Thus, in principle, these patients had healthy lungs. All CT-SPECT pairs could be matched with the lung contour method, without any problems. The time-consuming marker method was not applied for this large number of patients. In Figure 3, the optimal SPECT threshold (determined by iteratively performing chamfer matching) is plotted as a function of the maximum SPECT value in the thorax. As can be expected, the optimal SPECT threshold increases if the maximum SPECT value increases (Fig. 3). The data points could be fitted with a straight line through the origin (the slope was 0.37 ± 0.01, mean ± s.e.m.). The ratio of the optimal threshold and the maximum SPECT value was, for all patients, in the range of 0.23–0.53.

CT-CT

Comparison of the Two Methods. The average difference in the transformation between the conventional method (with anatomical markers and, occasionally, a manual shift) and the new method (lung contour match) showed no systematic differences (Table 2).

For CT-CT registration, the best match can be defined in several ways. First, the best match can be defined as the match with a minimal value for the cost function used in the chamfer matching algorithm (which is a measure for the RMS distance between the lung surfaces). In that case, the new method (lung contour match) is, by definition, better than the conventional method (marker/manual method).

Second, the best match can be defined as the match for which the nonoverlapping volume of the lungs is minimal. Therefore, we define the fraction of the volume that is nonoverlapping as:

$$f_{NOV} \equiv NOV_{AB}/(V_A + V_B), \qquad \text{Eq. 1}$$

TABLE 2
Average Transformation Between Manual Match and Lung Contour Match*

Parameter	CT-CT, before − after irradiation
Translation, mean ± s.e.m. (mm)	
ΔT_{AP}	0.3 ± 0.6
ΔT_{CC}	0.8 ± 0.9
ΔT_{RL}	0.0 ± 0.4
Rotation, mean ± s.e.m. (°)	
ΔR_{AP}	0.3 ± 0.5
ΔR_{CC}	−0.2 ± 0.3
ΔR_{RL}	−0.5 ± 0.6
No. of patients	20

*For each patient, the pre- and post-treatment CT scans were matched with the two methods, yielding two transformations for the post-treatment scan (the pretreatment scan was the template). The meaning of the numbers is similar to that as in Table 1: presented are the differences between the two transformations (three translations and three rotations, ΔT and ΔR, respectively), averaged for 20 patients. The indices denote the axis directions anterior → posterior (AP), caudal → cranial (CC) and right → left (RL). Also indicated are the s.e.m. values. The signs are defined so that the numbers represent the transformation (of the post-treatment scan) from the marker match situation to the lung contour match situation. If the marker match had been identical to the lung contour method, all values would be zero.

where V_A and V_B are the CT lung volumes of the pre- and posttreatment CT scans, respectively, and NOV_{AB} is the total, nonoverlapping volume. NOV_{AB}, V_A and V_B were determined from the segmented lungs, including the diaphragm. For a perfect overlap, f_{NOV} equals 0, and for totally mismatched lungs, f_{NOV} equals 1.

The nonoverlapping fraction f_{NOV} was determined for the 20 patients. For all except one patient, the lung contour method yielded a lower f_{NOV} than did the conventional method. This is also expressed in the difference between the fractions obtained with the conventional and the new method, $f_{NOV,conv} - f_{NOV,new}$, which is, on average, 2.3% ± 0.5% (mean ± s.e.m.) and significantly different from zero. The results indicate that, for CT-CT matching, the lung contour method is slightly better than the marker/manual method.

DISCUSSION

CT-SPECT

We implemented a method to match CT and SPECT scans of the thorax, based on aligning the lung contours in three dimensions. The method is fully automatic and fast and, therefore, easy and convenient to use.

It has been reported that irradiation of the lungs of up to 35–45 Gy induces a reduction in the SPECT signal up to 50% (*5,6*). Despite this fact, for healthy and partly irradiated lungs, the same, small systematic differences between the conventional and the new method were observed (Table 1). Thus, although the SPECT signal is highly reduced in the irradiated lung regions, no measurable influence of the radiation treatment could be detected on the matching performance.

Ventilation. The marker match method is expected to be less accurate than the lung contour method due to errors in the positioning of the markers, manually identifying the markers in the scans and skin–lung movement. On the other hand, it could not be ruled out a priori that, with the lung contour match, a systematic shift or rotation is introduced. Effects that could induce this are the breathing motion and the functional nature of the SPECT modality, e.g., the lung apices show less SPECT

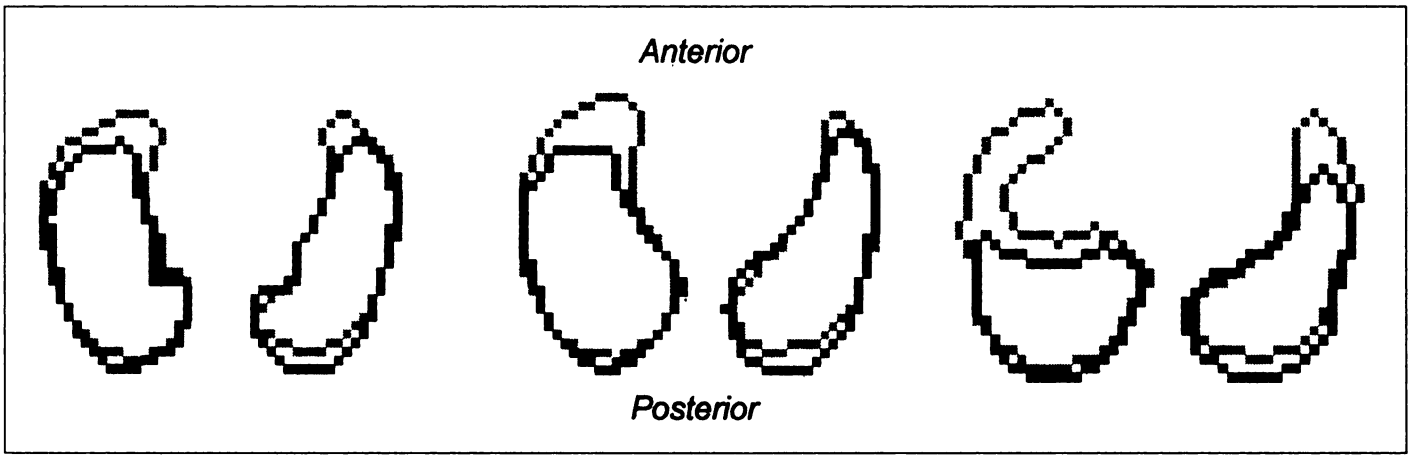

FIGURE 4. Effect of the gravity force on the SPECT scan. Lung contours extracted from the ventilation (gray) and the perfusion scan (black) in three transversal planes. The patient was in the supine position, and perfusion and ventilation were recorded simultaneously. The perfusion contours are located more posteriorly with respect to the ventilation contours.

signal than do other regions of the lungs (*13*). By comparison of the transformation matrices generated with the conventional and the lung contour method (Table 1), no obvious systematic shifts or rotations were observed, provided that the ventilation contours were used in the new method. Only one rotational difference was significantly different from zero ($\Delta R_{AP} = 0.9 \pm 0.2°$), for which we do not have a plausible explanation. On the other hand, the value is less than 1° and only significantly different from zero because the s.e.m. is small compared to other s.e.m. values (Table 1). Moreover, when a large number of values are reported, there is a large probability of finding a significant value by coincidence (for the other nonzero value, ΔT_{AP}, see below).

It is difficult to determine the accuracy of the new method, because, due to its inherent limitations, the marker match method can hardly be taken as a perfect standard. Phantom experiments could also not answer this question because their relevance is arguable for a moving organ, which can also differ in size (e.g., due to a difference in breathing level). It is clinically relevant to assess whether the accuracy of the new, automated method is at least comparable or maybe even better than the existing, conventional method. A good criterion to define the best match between CT and SPECT of the lungs could be that, for healthy lungs, the number of SPECT ventilation counts outside the CT-defined lung ($N_{outside}$) is minimal. Our results show that the amount of ventilation counts outside the CT-defined lung is slightly, but significantly, smaller with the new method than with the conventional method. This is the first indication that the new method is more accurate than the conventional method.

Inconsistency of the Marker Positions. A small shift in the AP direction was observed when the marker match was compared with the lung contour match based on the ventilation scan (ΔT_{AP} was approximately −2 mm, before and after irradiation; Table 1). This can be explained by the fact that the skin markers used in the SPECT scan cannot be regarded as point sources and by the differences in shape of the CT and SPECT couches.

Due to the 6.0-mm thickness of the disk-shaped container of each ^{57}Co source, the distance of each SPECT marker to the skin is 3.0 mm. This introduces an inconsistency in the marker positions of the SPECT and the CT scan. To verify this, the scans of the 11 patients for whom the SPECT marker on the back was visible on the scan were examined. For these patients, the one-dimensional distance in the AP direction between the back marker and one of the anterior markers (chest or abdomen marker) was, indeed, in the SPECT scan, 5 ± 2 mm larger than that in the CT scan. Furthermore, it was observed that this was also the case for the one-dimensional AP distance of the back marker and a lateral marker (left or right). This can be well explained by the shape difference of the couches used during SPECT and CT scanning. For SPECT, the patients were scanned on a hollow, and for CT, they were scanned on a flat couch. The hollow couch could easily lift the two lateral skin markers (i.e., move to the anterior direction) with respect to the lungs and the other markers.

Summarizing, in the SPECT scan, four of the five skin markers (and in half the patients, four of the four markers) are probably positioned too much anterior with respect to the lungs. This introduces an error in the marker match of 2–3 mm and quantitatively explains the AP translation difference between the two matching methods (ΔT_{AP} = approximately −2 mm). The latter shows that some shortcomings of the marker match method, incorrect positioning of the markers and moving of the skin with respect to the organ of interest can be demonstrated using the lung contour matching method. This is the second indication that the new method is better than the conventional method.

Optimal SPECT Threshold. The optimal SPECT threshold for segmenting the lungs from a ventilation SPECT scan was found at approximately 37% of the maximum number of counts (Fig. 3). Theoretically, this would be a better starting value for iteratively determining the optimal SPECT threshold than the fixed starting value of 200 counts, which we used until now. The relatively large range of the maximum count values is due to differences in the ^{81m}Kr concentration determined by the krypton generator and/or differences in the ventilation characteristics for each patient.

Perfusion and Gravity. When applying the lung contour method with the perfusion SPECT lung contours, a small systematic shift in the AP direction was detected (6–7 mm; Table 1) that appears to be consistent before and after radiotherapy. This AP shift corresponds to the observation that, for most patients in this study, the perfusion lung contours are located slightly posterior with respect to the ventilation lung contours (ventilation and perfusion are already matched because they are measured simultaneously), an example of which is given in Figure 4. The effect can be well explained by the gravity force, which has a larger influence on blood flow (perfusion) (*15,16*) than it does on air flow (ventilation). Consequently, when matching on the basis of the perfusion lung contours, an artificial shift of the SPECT scan is introduced in the posterior → anterior direction.

In clinical practice, occasionally, only a perfusion SPECT scan is measured. It can be argued that, in such cases, a gravity correction has to be made when the lung contour method is used. On the other hand, the observed shift for perfusion SPECT is comparable to the voxel size of the scan (6 mm) and much lower than the spatial resolution (20–25 mm FWHM). For an individual patient, it is, therefore, not clinically relevant to pursue a higher accuracy. However, when examining large groups of patients for research purposes, one may want to exclude all systematic errors. For a gravity correction, the simplest method is proposed, that is, to shift the SPECT perfusion scan after matching in the AP direction. The difference in AP translation between using the ventilation and the perfusion lung contours is 6 mm − 2 mm = 4 mm (Table 1).

CT-CT

Diaphragm. Both the CT and the SPECT scans were recorded during tidal respiration. It was necessary to omit the lung contours in the diaphragm region when matching CT-CT to avoid mismatches (e.g., totally misaligned trachea). In SPECT-CT matching, such mismatches were not observed (although the SPECT resolution is high enough to detect the trachea). The reason for this difference could be that the SPECT scan is a time average over many breathing cycles (typical acquisition time = 15 min), whereas a CT slice is recorded much more quickly (acquisition time = 1.0 sec). The correlation of two noisy signals (CT diaphragms) gives less accurate results than does the correlation of a noisy (CT diaphragm) and a smooth, averaged signal (SPECT diaphragm). A possible explanation is that RMS optimization is sensitive for outliers, which are mostly found in CT–CT correlation.

Comparison of the Methods. When the CT lung contours are aligned with internal markers and by manual shifting (conventional method), the operator is, in fact, minimizing the distance between the lung contours in three dimensions by eye. Therefore, it is expected that the automatic, new method is more accurate because a computer is more suitable for this job. The latter has been demonstrated by a lower nonoverlapping lung volume for the automated method.

Influence of Organ Shape. When comparing the accuracies in Table 1, it appears that, for the translation in the CC direction (ΔT_{CC}), the s.e.m. values are approximately twice as large as those for the translations in the other directions. The same observation can be done for CT-CT matching (Table 2). A possible explanation is that the resolution of the CT scans is much lower in the CC direction (10 mm) than it is in the AP and the RL directions (typically 2 mm). Alternatively, or additionally, the "cylindrical" shape of the lungs could be the cause of a larger degeneracy in the CC direction than in the other directions.

Future Applications and Suggestions. We are confident in applying the automated method on CT-SPECT match operations. Although no solid proof has been found that the new method is better than the conventional method, two indications that it is more accurate were found. Most important is that no large systematic shifts or rotations are introduced with this method. The merits of the new method (speed and convenience) are obvious.

A gold standard for a good CT-SPECT match could be found by using a SPECT transmission image. Gamma cameras are increasingly equipped with an external line source, which makes it possible to record a SPECT transmission scan simultaneously with the perfusion/ventilation SPECT scans. For future projects, it could be worthwhile to investigate whether CT-SPECT matches are significantly improved, when the CT lung contours are correlated with the lung contours extracted from this SPECT transmission image.

CONCLUSION

For CT-SPECT matching, a fast, automatic method has been developed on the basis of the lung contours and chamfer matching, without the use of external skin markers, and requires less than 2 min. When using the ventilation SPECT scan for matching, the method does only introduce a negligible systematic shift and rotation with respect to a conventional method with external skin markers. The systematic shift can be ascribed to an inconsistency of the marker positions in the latter method. The new method is at least as accurate as the conventional method. The results for healthy and partly irradiated lungs are very similar. When the perfusion scan is used for matching instead of the ventilation scan, the scan has to be shifted by a small amount (4 mm) in the AP direction. This accounts for the effect of gravity on the blood flow.

For CT-CT matching, with the scans recorded under tidal respiration, the slices of the diaphragm have to be removed to reliably correlate the lung contours. The method is slightly more accurate than a manual method using anatomical landmarks.

ACKNOWLEDGMENTS

We thank Dr. R.W. de Boer for useful discussions and Drs. H. Bartelink, B. Mijnheer and R.A. Valdés Olmos for critically reading this manuscript. This work was supported by a Dutch Cancer Society Grant NKI 94-819.

REFERENCES

1. Goldenberg DM, Larson SM. Radioimmunodetection in cancer identification. *J Nucl Med* 1992;33:803–814.
2. Larson SM, Divgi CR, Scott AM. Overview of clinical radioimmunodetection of human tumors. *Cancer* 1994;73:832–835.
3. Weber DA, Ivanovic M. Correlative image registration. *Semin Nucl Med* 1994;24: 311–323.
4. Marks LB, Spencer DP, Sherouse GW, et al. The role of three-dimensional functional lung imaging in radiation treatment planning: the functional dose-volume histogram. *Int J Radiat Oncol Biol Phys* 1995;33:65–75.
5. Boersma LJ, Damen EMF, De Boer RW, et al. Dose-effect relations for local functional and structural changes of the lung after irradiation for malignant lymphoma. *Radiother Oncol* 1994;32:201–209.
6. Marks LB, Munley MT, Spencer DP, et al. Quantification of radiation-induced regional lung injury with perfusion imaging. *Int J Radiat Oncol Biol Phys* 1997; 38:399–409.
7. Pelizzari CA, Chen GTY. Registration of multiple diagnostic image scans using surface fitting. In: Bruinvis IAD, van der Geissen PH, van Kleffens HJ, Wittkämper FW, eds. *The use of computers in radiation therapy*. Amsterdam: Elsevier; 1987:437–440.
8. Kessler ML, Pitluck S, Petti P, Castro JR. Integration of multimodality imaging data for radiotherapy treatment planning. *Int J Radiat Oncol Biol Phys* 1991;21:1653–1667.
9. Jiang H, Holton K, Robb RA. Image registration of multimodality three-dimensional medical images by chamfer matching. *Proc. SPIE Biomed Image Process* 1992;1808: 356–366.
10. Mangin JF, Frouin V, Bloch I, Bendriem B, López-Krahe J. Fast nonsupervised three-dimensional registration of PET and MR images of the brain. *J Cerebr Blood Flow Metab* 1994;14:749–762.
11. van Herk M, Kooy HM. Automatic three-dimensional correlation of CT-CT, CT-MRI, and CT-SPECT using chamfer matching. *Med Phys* 1994;21:1163–171.
12. Yu JN, Fahey FH, Gage HD, et al. Intermodality, retrospective image registration in the thorax. *J Nucl Med* 1995;36:2333–2338.
13. Damen EMF, Muller SH, Boersma LJ, De Boer RW, Lebesque JV. Quantifying local lung perfusion and ventilation using correlated SPECT and CT data. *J Nucl Med* 1994;35:784–792.
14. Gilhuijs KGA, van Herk M. Automatic on-line inspection of patient set-up in radiation therapy using digital portal images. *Med Phys* 1993;20:667–677.
15. Gattinoni LG, Pelosi P, Vitale G, Pesenti A, D'Andrea L, Mascheroni D. Body position changes redistribute lung computed-tomographic density in patients with acute respiratory failure. *Anesthesiology* 1991;74:15–23.
16. Verschakelen JA, van Fraeyenhoven L, Laureys G, Demedts M, Baert AL. Differences in CT density between dependent and nondependent portions of the lung: influence of lung volume. *Am J Roentgenol* 1993;161:713–717.